Geochimica et Cosmochimica Acta Vol. 48, pp. 343–360

0016-7037/84/$3.00 + .00

Studies of an artificially shock-loaded H group chondrite

D. W. SEARS

Department of Chemistry, University of Arkansas, Fayetteville, Arkansas 72701, and Department of Physics, University of Birmingham, Birmingham, B15 2TT, UK

J. R. ASHWORTH and C. P. BROADBENT

Department of Geological Sciences, University of Aston in Birmingham, Gosta Green, Birmingham, B4 7ET, UK

and

A. W. R. BEVAN

Department of Mineralogy, British Museum (Natural History), Cromwell Road, London, SW7 5BD, UK

(*Received March* 15, 1982; *accepted in revised form November* 17, 1983)

Abstract—Five samples of the naturally unshocked Kernouve (H6) meteorite were artificially shock-loaded to pressures of 70, 165, 270, and 390 kbar and the silicates and metal examined optically, by scanning and transmission electron microscopy and by thermoluminescence (TL). Olivine deformation is closely comparable to that in naturally shocked meteorites, producing dislocations with Burgers vector [001]. At pressures of ≤165 kbar, these are formed in well-defined slip planes. At 270 kbar, olivine develops optical mosaicism, has high dislocation densities throughout and is also highly fractured. Recovery, due to heating is minimal. In orthopyroxene, the deformation mechanism changes, from the clino-inversion to unit-dislocation slip, between 70 and 165 kbar. In diopside, (001) and (100) twinning was produced. Plagioclase is inferred to have been progressively converted to maskelynite, but some is still present in 270 kbar sample.

The microhardness of the kamacite in the samples increases with shock pressure. The $\alpha \rightarrow \epsilon$ transformation pressure in the kamacite is 30–40 kbar higher than observed for iron meteorites. Annealed kamacite displays incipient polycrystallinity and α-martensite and taenite sometimes contains slip lines. Troilite acquired cracks, undulose extinction, twins, polycrystallinity and finally melted as the shock pressure increased.

At pressures over 200 kbar there was a systematic decrease in the natural TL and the TL sensitivity. Detailed considerations of changes in the natural TL/TL sensitivity ratio for various regions of the TL glow curve suggest that two processes were effective during shock; thermal drainage of electron traps and a reduction in the effective trap density. It is suggested that the latter process associated with the vitrification of feldspar, the TL phosphor.

An additional sample was subjected to a shock pulse which was "spiked" instead of square. Very distinctive changes were apparent; thermal effects are conspicuous and with widespread annealing (~600–800°C) of metal and sulfide. Glassy, opaque veins were produced which are analogous to the black veins in shock-lithified gas-rich meteorites. Anomalous low-temperature TL was induced, suggesting that a new or modified phase or mineral has become the dominant TL phosphor.

INTRODUCTION

THE LONG AND enigmatic history of meteorites is marked by several major episodes: each left its mark on isotopic properties, on petrology and to varying extents on their chemistry. Three of these major episodes are condensation and accretion in the primitive solar nebula, long-term static metamorphism in reasonably large parent objects and dynamic metamorphism due to some violent shock events. This paper concerns the last of these three events.

There is considerable literature on the effect of shock on meteorites. It seems to have been associated with the break up of parent bodies (HEYMANN, 1967; TURNER *et al.*, 1978; BOGARD *et al.*, 1976), with a period of regolith activity of gas-rich meteorites (*e.g.*, DODD, 1969) and with some very early stage in the history of unequilibrated ordinary chondrites; it may even have been the sole cause of the highly variable degree of metamorphism displayed by type 3 chondrites (HUSS *et al.*, 1981; HUSS, 1980; SEARS and MARSHALL, 1980; SEARS *et al.*, 1980). Clearly, it is an important aspect in the history of meteorites. With some justification, DODD and JAROSEWICH (1979) suggest that a shock indicator be added to van Schmus and Wood's two-dimensional classification scheme for chondritic meteorites.

Shock is a frequently invoked phenomenon in interpreting meteorite properties, although on many occasions, too little is known about the nature of shock effects for such interpretations to be very satisfying. Although much work has been published concerning shock effects in lunar and terrestrial samples, studies of artificially shocked chondrites, with their unique mineral assemblages, are very few. FREDRICKSSON *et al.* (1963) briefly described petrologic changes in two artificially shocked chondrite samples and LIENER (1966) made some TL observations on this material. The present work reports an investigation by three laboratories on meteorite material which has been artificially shock loaded to pressures up to 390 kbar or more. Our studies involve silicate mecropetrography with transmission electron microscopy, metallographic and thermoluminescence measurements. Of course, these studies do not represent a comprehensive coverage of meteorite properties, but they are three very

different solid state phenomena which are highly sensitive to shock effects. Their collaborative application has allowed new insights into the behavior of meteorite material under dynamic loading.

EXPERIMENTAL

Material and shock loading experiments

The Kernouve H6 chondrite was chosen for the experiments for two reasons. We wanted an H chondrite so that our results could be used with comparable data being culled by Robert Hutchison's H chondrite consortium. We also obviously wanted a meteorite showing no natural shock effects other than ubiquitous features like Neumann bands. Kernouve also has an extremely old ^{39}Ar-^{40}Ar age (4.47 ± 0.5 Ga), suggesting that it has remained essentially unaltered since its formation and cooling (TURNER *et al.*, 1978). Hutchison made 69 g available, from British Museum (Natural History) specimen BM44143, for this and related studies. The shock experiments were performed by R. L. Gyton and K. D. Burrows of the Atomic Weapons Research Establishment, Foulness. With their advice the following sample preparation was adopted. Six 2×0.5 cm discs of Kernouve were prepared and the offcuts carefully documented to serve as controls. The discs were placed in recesses in blocks of aluminum alloy (HE-30), 200 mm in diameter and 200 mm deep. This alloy was chosen because its shock characteristics are thought to closely resemble those of the samples. A pool of araldite resin was then poured over the sample and block and the assembly placed in a chamber and evacuated. The system was allowed to pump down until air had ceased to degas but before the resin started to boil. The vacuum was then released and a cap was slid under the resin and into the recess. Once set, the billet was lathed off until a 1 mm thick cap of Al remained. Great pains were taken to minimize the amount of resin trapped in the container by grinding the meteorite discs to fit tightly into the blocks. Later investigation showed that the operation was successful and also that there was no impregnation of the compact meteorite by the resin.

The shock loading was performed with a 75 mm disc of high explosive, carefully machined flat and parallel on both faces. This was uniformly detonated over its back surface (Fig. 1) and used to throw a flat steel plate across a small air gap, giving plane impact with the meteorite samples. Maximum shock pressure and duration were adjusted by varying amount and type of explosive, the flying plate thickness and the stand-off distance. Three explosive types, 15–40 mm thick, and plates varying between 3 and 9 mm were used, with stand-off distances between 12.5–26 mm. Recovery of material was generally difficult, and it was found necessary to add securing plates to the front of the sample; 1 mm thick steel was used for the low pressure shots and 6.5 mm thick copper was used for the high pressure shots. A piezo-resistive Manganin gauge was sandwiched between this plate and the sample block in order to record the pressure profile.

Samples were shock loaded to pressures of 70, 165, 270 and 390 kbar,* where each pressure is believed to be within ±5% of the value quoted; this is the pressure wave entering the sample. The pressure experienced by the meteorite would have attenuated with depth and would have varied throughout the sample due to the complex interaction between the shock-wave, rarefaction wave and grain boundaries. As a consequence, the uncertainty on the pressure determination experienced by a sample is probably about ±20% (D. STÖFFLER, pers. commun.). We emphasize that our experimental conditions are less well characterized than is usual for simple monominerallic tests on thin samples, but we suggest that they more closely match the conditions experienced by heavily shocked meteorites. We have made several observations which would not have been possible with monominerallic samples. An additional sample was subjected to a higher pressure, but because of experimental changes in the experimental procedure required to achieve this pressure and have acceptable recovery, it proved difficult to calculate the size of shock. All our data seem to indicate a value of >400 kbar for this sample. The main feature of this shock experiment was that it resulted in a pulse which dropped more rapidly with time, than the earlier experiments. We will refer to this sample as the "spike-shocked" sample. It is fortunate that the amount of recovered material is very high, because in all our studies this sample proved to be particularly interesting.

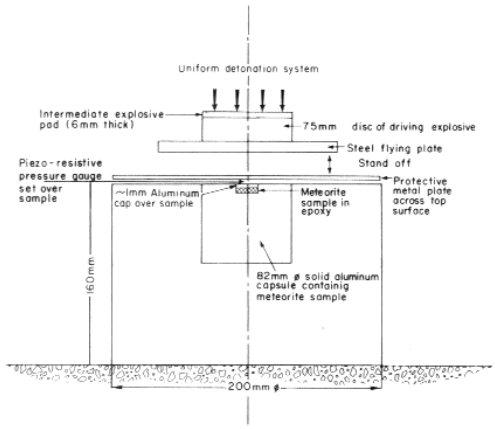

FIG. 1. Sketch showing the shock loading assembly. Not to scale.

100–200 mg samples from each shock pressure were used for each of TL, HVEM and metallographic observations, except for the 390 kbar sample for which the recovered mass was extremely small (~100 mg). This sample was crushed, the magnetic material removed for metallographic work and the homogenized powder was divided equally for TL and HVEM work.

Transmission electron microscopy

All samples except the 390 kbar powder were made into doubly-polished thin-sections for optical examination, and then prepared for high-voltage electron microscopy (HVEM) by ion-beam thinning of selected areas. Except for the spike-shocked sample, all were friable and needed impregnation prior to sectioning. The spike-shocked sample was dark in color and nonfriable. Fine particles from the 390 kbar powder were collected as "dust" on a glass slide, which was then carbon-coated, and the carbon coating stripped and transferred with its embedded grains to grids for HVEM, without further treatment. The high-voltage electron microscope was operated at 1 MV with a double-tilt stage. Minerals are identified, and their orientations characterized, from electron diffraction patterns of selected small (~1 μm^2) areas.

Chemical etching of olivine

Rather low dislocation densities were anticipated in samples from the mildest shock experiments, so we also prepared three polished thin-sections, for chemical etching and examination, by optical means and by scanning electron microscopy (SEM); one each from the 165 kbar, 70 kbar and unshocked samples. This enabled study on a coarser scale than can be achieved by HVEM. An olivine etchant was

* These values have been rounded-off slightly, but within errors, from the values quoted in a previous paper that referred to these samples (SEARS, 1980).

selected, because olivine is the most abundant mineral and its deformation behavior is relatively simple. WEGNER and CHRISTIE's (1974) etchant No. 6 was used, for 50 seconds, at room temperature. The cleaning procedure described by these authors was followed and the specimens were coated with a thin film of palladium-gold. In olivine grains with

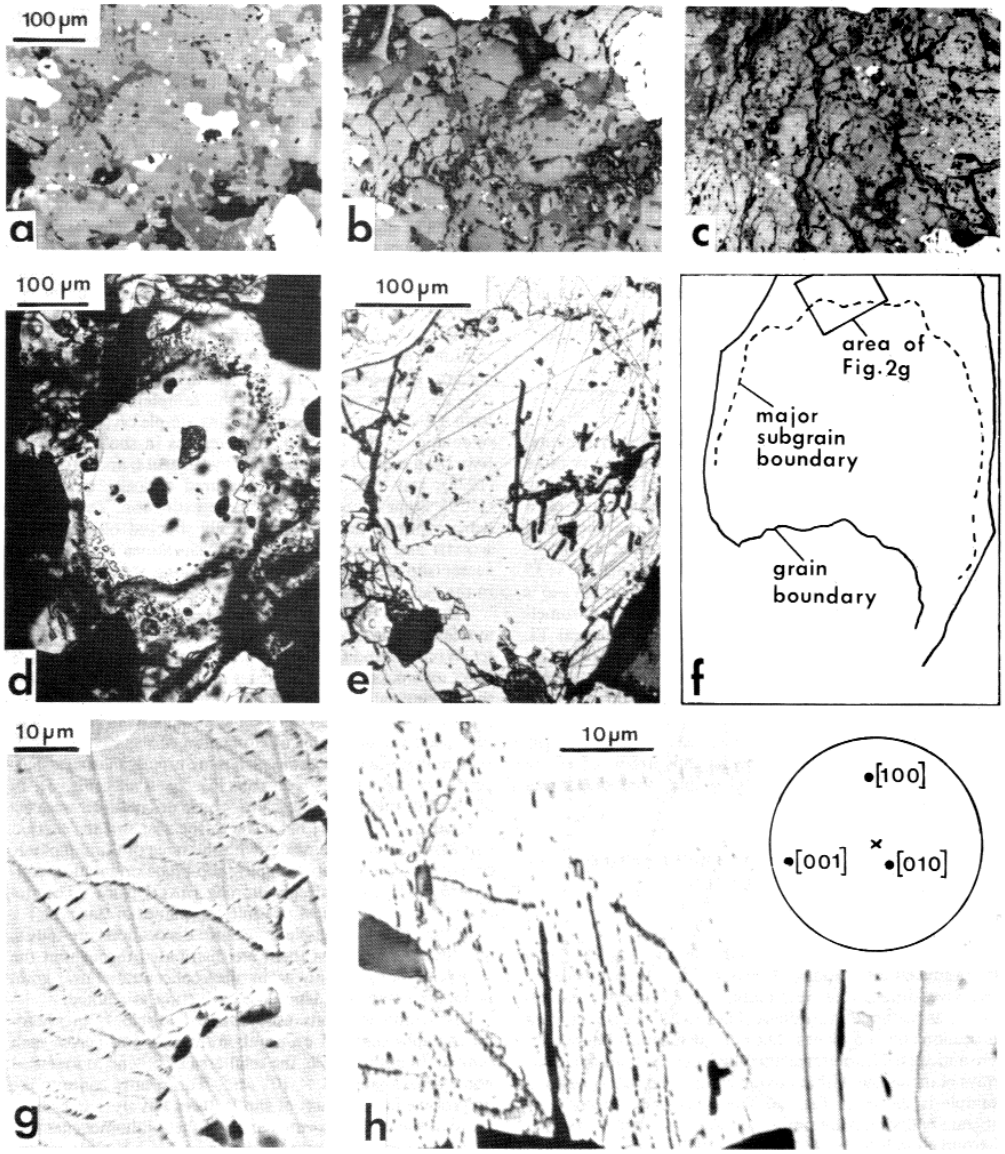

FIG. 2. (a)–(c) Reflected-light micrographs of typical areas in polished surface showing progressive fracturing due to shock. Bright grains are metal or sulphide, grey areas are silicate or epoxy impregnating resin, and black areas of pit produced during specimen preparation. (a) unshocked Kernouve. Light grey is olivine or pyroxene, darker grey, interstitial plagioclase. (b) 70 kbar sample, showing abundant fine cracks in the silicates. (c) 270 kbar sample, showing intense fracturing. Many broad cracks are filled by epoxy resin. (d)–(h) Naturally-occurring dislocations in Kernouve olivine. (d) transmitted light photomicrograph showing a curved array of inclusions sub-parallel to the outer boundary of a grain, interpreted as a particles "decorating" a subgrain boundary. (e)–(g) a curved, decorated subgrain boundary in unshocked Kernouve, revealed by etching the individual dislocations. Etch pits appear dark; linear grey features are etched polishing scratches. (e) reflected light, showing the relation between the subgrain boundary and opposite boundaries of the grain, as further clarified in the sketch (f). (g) SEM, showing minor subgrain boundaries emanating from the major one, and scattering dislocations, in the rim of the grain. (h) sets of sub-parallel dislocation arrays; reflected light.

particularly interesting features, the crystallographic orientation of the surface plane was subsequently estimated by transmitted-light optics using a universal stage, and the crystal orientations are represented in upper-hemisphere stereographic projection.

Metallographic studies

Samples were impregnated and mounted in epoxy resin, then ground, polished and etched with 2% nital for 10 seconds for metallographic observation. Microhardness measurements were made with a Vickers microscope and indenter. Penetration under a load of 100 grams for 15 seconds was measured as the diagonal lengths (Vickers Hardness Number, VHN). Green light was employed and only those indentations with regular outlines and without extensive cracking were used. Large cracks were avoided and, where possible, measurements were taken more than one indentation width from grain boundaries. In general we attempted to make measurements at the cores of large grains (200–300 μm), but this was not always possible with taenite grains which are usually smaller than $\sim$50 μm. For this reason our data for taenite (HV_γ) are inferior to those for kamacite (HV_α).

Thermoluminescence studies

The sample preparation procedure and the experimental apparatus for the TL measurements were the same as those described by MILLS *et al.* (1977). Briefly, this consists of heating the sample in an inert atmosphere at a carefully controlled rate of 5°C/sec. The samples were in the form of fine-grains deposited on Al disks in the manner described by SEARS (1980). The light output was measured with an EMI 9635 QB photomultiplier tube, amplified and plotted on the y-axis of a plotter with temperature, as measured by a chromel-alumel thermocouple, on the x-axis. After the natural TL had been recorded, and therefore removed, the samples were given a dose of 50 krad by exposure to a ^{60}Coγ source with a dose rate of 1.4 Mrad/h and resulting TL recorded. In this way it is possible to measure the ability of the samples to respond to radiation. In this paper we refer to the maximum TL emission observed in the powder thus irradiated as the "TL sensitivity" and the glow curve thus produced as the "induced TL".

OPTICAL, SEM AND HVEM OBSERVATIONS ON THE SILICATES

Olivine

The shock experiments cracked the silicates (Fig. 2a–c) and also produced dislocations in olivine (Fig. 3). In unshocked Kernouve, dislocations were found only in subgrain boundaries or as scattered individuals (Fig. 2d–h), as distinct from dislocations on slip planes. The curved subgrain boundaries were anticipated from transmitted-light observations of curved arrays of inclusions within olivine grains (Fig. 2d). An etched example is shown in Fig. 2e. These naturally "decorated" subgrain boundaries are similar to those described from other H-group chondrites by ASHWORTH (1979a), where the decorating particles are exsolved chromite grains. In Kernouve, some of the decorating particles are transparent and colorless, similar to those found by CHRISTOPHE (1979) in the Sena H4-5 chondrite. Some subgrain boundaries are sub-parallel to the exterior boundary of the host grain (Fig. 2d, e, f); in particular, Fig. 2e displays a phenomenon described by CHRISTOPHE (1979, p. 412) using a different technique in Sena, where a dislocation-poor olivine core is separated by a major, decorated subgrain boundary, from a rim containing numerous "growth dislocations". In the present case, the growth dislocations are concentrated in minor subgrain boundaries (Fig. 2g). Thus a two-stage growth history is deduced for this grain, and suspected for others from the distribution of inclusions (*e.g.*, Fig. 2d). In Kernouve, which has low porosity (CHRISTOPHE, 1978), it is not possible to study grain morphologies produced by the second stage; in the more porous Sena, CHRISTOPHE (1979, p. 414) suggests on the basis of the crystal forms that growth was from a vapor phase.

A different kind of subgrain boundary is found as sub-parallel sets at a high angle to [001] (Fig. 2h). These are identified as subgrain boundaries, rather than slip planes, from their sinuous shape and the fact that they do not contain the vector [001] which is the predominant slip vector (see below). They may represent the effect of annealing at high temperature after an early deformation, the interpretation offered for closely-spaced subgrain boundaries in this type of orientation in Saint-Severin (ASHWORTH and BARBER, 1977). It is noteworthy that, in the Kernouve material, they are rare.

Etching confirms that olivine in the natural Kernouve material lacks slip dislocations of shock origin. Slip planes are found only in the artificially shocked samples (Fig. 3). In the 70 kbar sample, they were seen only locally, mostly at the edge of the sample, near the aluminum holder. Slip planes generally do not extend all the way across a grain (Fig. 3). In Fig. 3a they die out laterally away from the nearby aluminum holder. In Fig. 3c, they are contained in a band within a grain. Elsewhere, olivine appears merely to have cracked (Fig. 2h is from such an area of this sample). Cracks tend to form sub-parallel sets approximating simple crystallographic orientations. The orientations of cracks in shocked olivine have been studied systematically by REIMOLD and STOFFLER (1978), and their densities measured optically by BAUER (1979). Some olivine has undulose extinction. The HVEM work confirms that, as in naturally shocked olivine (ASHWORTH and BARBER, 1975), the dislocations have Burgers vector (slip vector) b = [001] and have long, straight segments in the "screw" direction [001] (Fig. 4a).

The shapes of etch pits (Fig. 3) bear no obvious relation to this direction, and must be attributed to anisotropic etching (*cf.* WEGNER and CHRISTIE 1974). In the present study, the effect on cracks (Fig. 3) indicates that the etching rates in the three principal crystallographic directions are in the order [010] > [100] > [001]. This effect alone appears to be sufficient to explain the directions of elongation of the etch pits. It is evident that slip dislocations etch more rapidly than subgrain-boundary dislocations (compare Fig. 2g, h with Fig. 3). In all three of the deformed grains whose orientations were estimated (Fig. 3), [001] lies close to the plane of the section and approximately coincides with the trace of the slip plane, consistent with a steeply dipping slip-plane orientation containing [001], *i.e.*, a steeply dipping $\{hKO\}$ plane. (The stereograms in Fig. 3 show possible slip planes of this type.)

In the 165 kbar sample, more slip dislocations are found, and the grains bearing them are distributed throughout the sample. Dislocations are again often concentrated near grain boundaries (Fig. 3d). Undulose extinction was noted.

Dislocation etch pits were counted (Table 1) in photomicrographs centered on points forming a grid across each sample. In each sample, the total area of olivine represented was approximately 3×10^4 μm^2. The results confirm the progressive introduction of slip features but are unrepresentative of the most deformed areas of these inhomogeneously deformed samples: where closely spaced in a slip plane, dislocations may not be separately resolvable optically, as shown by SEM imaging (compare Fig. 3b with Fig. 3a) and indicated by HVEM observations of very close spacings (Fig. 4a). Moreover, the specimens contained voids produced by etching and subsequent disintegration: the amount of olivine remaining, estimated by point-counting as a percentage of total surface area including voids (Table 2) indicates the loss of highly deformed areas from the 165 kbar sample in particular. Etching studies were not feasible in the more heavily shocked specimens.

In the 270 kbar material, olivine is optically anomalous, failing to extinguish properly and having a "mottled" appearance, generally called mosaicism (CARTER *et al.*, 1968).

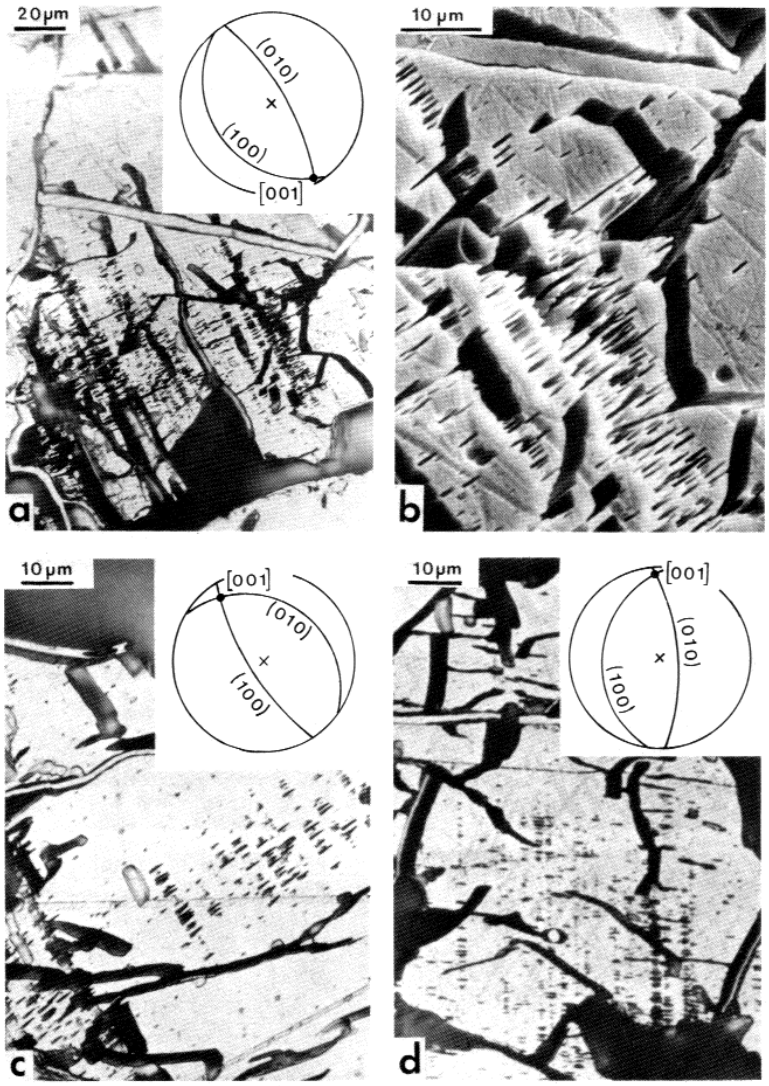

FIG. 3. Etched slip-plane dislocations and cracks in olivine in artificially shocked Kernouve. Some of the larger cracks contain epoxy impregnating resin. Large black areas are voids introduced artificially through etching and disintegration. (a) 70 kbar sample, reflected light. (b) part of the same area in SEM. (c) 70 kbar, reflected light, showing slip planes confined to an area within a grain. (d) 165 kbar, reflected light.

These authors use it to distinguish "heavily" from "moderately" shocked olivine. It has been attributed to a combination of plastic deformation (dislocation slip) and fracture (BAUER, 1979). The lattice misorientations give measurable effects in X-ray diffraction (HORZ and QUAIDE, 1972): domain size decreases with increasing shock pressure but may not be homogeneous. Our HVEM observations indicate that sharp misorientations on a scale comparable to the optical mottling (~ 10 μm) are generally due to cracks (Fig. 4b). High dislocation densities (often >30 μm^{-2}) are also pervasive, and cause more gentle bending. Screw dislocations with b = [001] are predominant, but some lines have "edge" segments (perpendicular to b) within the slip plane, giving a rectangular configuration as shown in an oblique view in Fig. 4c (*cf.* ASHWORTH and BARBER, 1975; ASHWORTH, 1981). In this example the slip plane is (010). Some dislocations with b = [100] were also found (*cf.* ASHWORTH, 1981).

The 390 kbar HVEM sample comprises fragments, mostly ~ 10 μm in size, with angular outlines attributed to disintegration along crystallographically controlled cracks (Fig. 4d). There are high densities of dislocations with b = [001].

Olivine in the spiked-shock specimen similar has high dislocation densities, and shows optical mosaicism.

Orthopyroxene

In the 70 kbar sample, orthopyroxene has been deformed by the mechanism that is most familiar in natural shock deformation, producing lamellae in (100) orientation. From other studies, these are known to have the clinoenstatite structure and widths that are multiples of the clinopyroxene lattice periodicity, approximately 9 Å; they will be called clino-lamellae (*cf.* ASHWORTH, 1980a).

Figure 4e illustrates a grain that was optically noted to

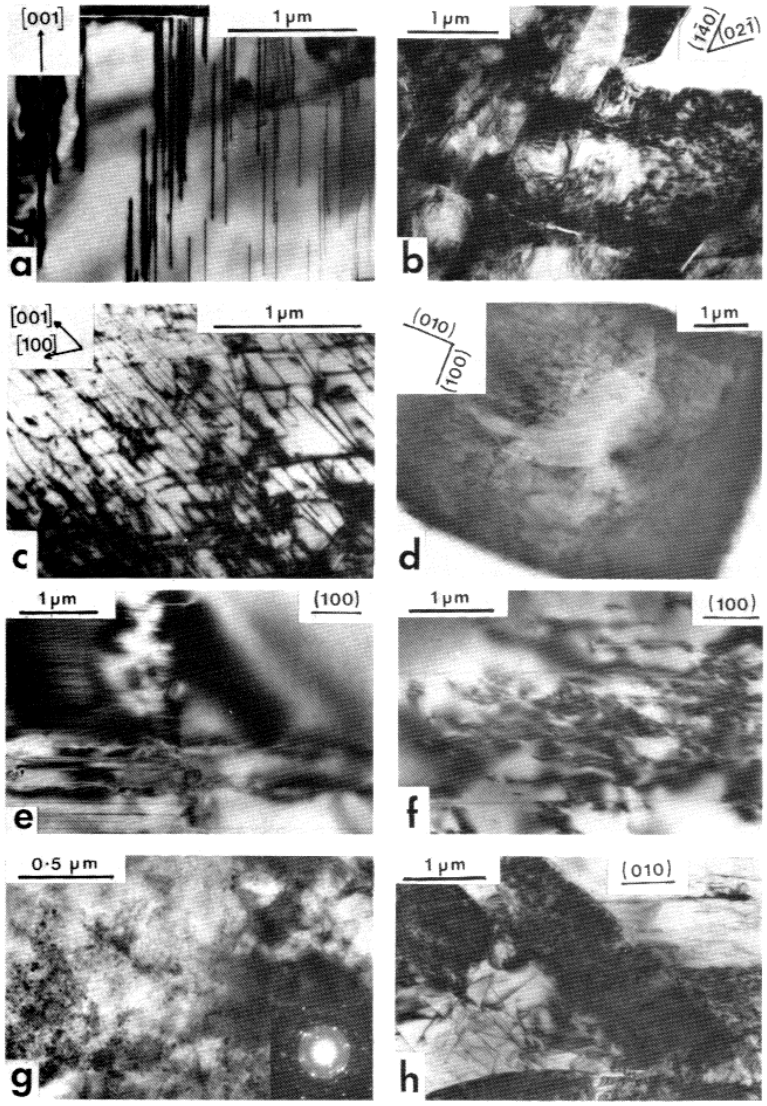

FIG. 4. HVEM photomicrographs of olivine (a–d) and orthopyroxene (e–h) in artificially shocked Kernouve. (a) dislocations in slip planes in olivine, 70 kbar sample, viewed approximately along the zone axis [210]. (b) high dislocation density and cracks in olivine, 270 kbar. The blocky appearance is due to small changes in lattice orientation across cracks (mosaicism). (c) slip dislocations in olivine, 270 kbar; viewed approximately along [213]. (d) an olivine fragment in the 390 kbar powder, showing crystallographically simple boundaries and internal dislocations. (e) inhomogeneously distributed clino-lamellae in orthopyroxene, 70 kbar; viewed approximately along [011]. (f) unit dislocations, and a few clino-lamellae, 165 kbar; viewed approximately along [012]. (g) heavily deformed edge of an orthopyroxene grain, 165 kbar. Inset diffraction pattern from the area at the left shows rings from finely crystalline material. (h) part of an orthopyroxene grain viewed approximately along the normal to the (100) plane, in the 270 kbar sample. The blocky effect is due to crack-induced mosaicism. Many dislocation lines have intricate shapes (left); some lie in a (010) plane (upper right).

have bands of slightly differing birefringence. The distribution of clino-lamellae is very inhomogeneous, and is undoubtedly due mostly to the artificial deformation. Two clino-lamellae crossing the relatively undeformed area are notably broad; contrast variations around them are due to the presence in their boundaries of many partial dislocations marking discrete changes in lamella width (*cf.* ASHWORTH, 1980a). These two clino-lamellae may well predate the experimental deformation.

As well as partial dislocations in the boundaries of clino-lamellae, there are a few unit dislocations—dislocations whose Burgers vector is a unit lattice vector, which occur outside the clino-lamellae.

Motion of unit dislocations on (100) slip planes, and motion of partial dislocations to generate (100) clino-lamellae, are alternative deformation mechanisms in orthopyroxene (RALEIGH *et al.*, 1971). Progressive operation of the partial-dis-

Table 1. Optical counting data for etched olivine.

Sample	Olivine as percentage of sample surface after etching	Measured etch-pit densities mm^{-2} slip-plane range	slip-plane average	other range	other average
unshocked	28.5	0	0	$(0\text{-}2.6)\times10^4$	1.7×10^4
70 kbar	22	$(0\text{-}2.6)\times10^4$	0.3×10^4	$(0.5\text{-}1.8)\times10^4$	1.0×10^4
165 kbar	11.5	$(0\text{-}7.8)\times10^4$	2.0×10^4	$(0.6\text{-}4.5)\times10^4$	1.5×10^4

location mechanism produces regions of untwinned clinopyroxene (COE and KIRBY, 1975). It has been inferred that this mechanism is common in natural shock-deformation of meteorites (REID and COHEN, 1967; ASHWORTH and BARBER, 1976a), which is consistent with the experimental evidence that the mechanism is favored by low temperatures, and by high strain rates, at least up to 10^{-3} s^{-1} (RALEIGH *et al.*, 1971). However, it has recently been suggested that intense shock pressure can activate the unit-dislocation mechanism (NORD and MCGEE, 1979). This in turn suggests that the predominance of the other mechanism in many meteorites may be useful in placing constraints on their shock histories. In this context, it is very interesting that the unit-dislocation mechanism is found to predominate in the present 165 kbar and 270 kbar samples. The effect is most obvious in the least strained parts of the 165 kbar sample, where individual dislocations and clino-lamellae are easy to resolve. The area shown in Fig. 4f is representative. This orthopyroxene has only a few, narrow clino-lamellae but many unit dislocations, clearly indicating the operation of unit-dislocation slip.

Some fine-grained material (Fig. 4g, left) is thought to have crystallized from the amorphous state following localized grain-boundary melting, since vesicles are locally apparent (Fig. 4g, top right). The ring diffraction pattern is consistent with clinopyroxene rather than orthopyroxene; the monoclinic form, as the end product of crystallization following shock-vein formation in orthopyroxene, has been described in coarser-grained form from natural occurrences (ASHWORTH and BARBER, 1976b, Fig. 1b; PRICE *et al.*, 1979, Fig. 1a and p. 214).

In the 270 kbar sample, intense deformation of orthopyroxene is pervasive. Clino-lamellae are visible where a grain is viewed at a high angle to [100]. A crystal viewed down [100] shows complex arrangements of dislocations (Fig. 4h). They are in strong contrast with the 00*l* diffraction row operating, indicating that the Burgers vector is in that direction, and there is a tendency for some of them to be aligned on (010) planes, indicating that the slip system (010) [001] has operated in addition to (100) [001]. ROSS and NIELSEN (1978) have reported (010) [001] slip under severe experimental conditions.

In the 390 kbar powder, only one grain of orthopyroxene was seen. It gave normal (though mosaicked) orthopyroxene diffraction pattern, and was internally intensely deformed.

Diopside

A Ca,Mg-rich clinopyroxene, loosely termed diopside, is a minor phase in Type 6 chondrites such as Kernouve. Twinning was generally produced on both (100) and (001) planes, even in the 70 kbar sample, indicating shock conditions more severe than those necessary for the production of (100) twins alone (ASHWORTH, 1980b).

Plagioclase

Shocked plagioclase often shows mosaicism (HORZ and QUAIDE, 1972) and twinning (AVE LALLEMANT and CARTER, 1972). It is converted to a diaplectic glass (maskelynite) more readily than are olivine and pyroxene. In single-crystal experiments, this transformation has been found to require peak pressures of 250–300 kbar (STOFFLER and HURNEMANN, 1972; STOFFLER, 1974; GIBBONS and AHRENS, 1977; OSTERTAG, 1981). An interesting feature of the present study is that local maskelynite production is inferred from HVEM observation in even the most lightly shocked specimen (70 kbar). Both glass and plagioclase (undeformed or with cracks and micro-twins) were found in this specimen, and in the 165 kbar and 270 kbar specimens. Only glass was found in the spiked-shock specimen. This glass is internally featureless, and is thus distinguished from melt veins (next section). Interdigitations of glass and plagioclase were not found, but the featureless glass is confidentially identified as maskelynite since plagioclase is the only mineral present that is easily vitrified. The inhomogeneity of the effect at 70–165 kbar prevents estimation of the proportion of plagioclase affected. This inhomogeneity is undoubtedly due to the effect on shock-wave propagation of the polycrystalline and polymineralic nature of the specimen. Rarefactions and reflections at grain boundaries cause peak pressures to be locally higher and locally lower than the experimentally established (equilibrium) pressure: this effect explains coexistence of plagioclase and maskelynite (HANSS *et al.*, 1978). Moreover, plagioclase, having a low acoustic impedance, will locally suffer severe compression in the polymineralic rock (SCHAAL *et al.*, 1979). The equilibrium pressure for onset of maskelynite formation is slightly lower in basalt (SCHAAL *et al.*, 1979) than in single-crystal plagioclase. Porosity introduces a strong inhomogeneity and further lowers the equilibrium pressure for the reaction (SCHAAL *et al.*, 1979; *cf.* KIEFFER *et al.*, 1976). Kernouve has 4 percent void space according to CHRISTOPHE (1978) and also, inevitably, some natural cracks, both of which must contribute to the inhomogeneity of compression. It is inferred that, even in the 70 kbar specimen, plagioclase *locally* experienced peak pressures above 250 kbar, while some parts of the 270 kbar specimen did not.

High-temperature effects in the spiked-shock specimen

This sample is particularly interesting in being indurated and blackened. Whereas all the other samples disintegrated during experimental deformation, to an extent that increases with increasing peak pressure, a cementing process was able to act on the spiked-shock material—presumably because of the different experimental parameters in this run.

The dark color of the bulk sample is due to veins and pockets that are opaque in thin-section. In polished surface, the reason for opacity is seen to be the presence of numerous small, opaque particles (Fig. 5a, b). The veins fill cracks in silicates and in chromite. Some have "schlieren" features indicating flow (*cf.* RAMDOHR 1973, Fig. E17). The melt pockets range up to 500 μm across. Some of the included opaque particles are irregular in shape (Fig. 5a), others are spherical droplets (Fig. 5b) of metal, sulphide and metal + sulphide, up to 50 μm across. Their internal structures cannot be clearly resolved optically. The metal particles are confirmed by electron-probe to consist mostly of Fe. This is worth mentioning because, in some shock experiments, globules of metallic melt have been incorporated into the sample from the metal holder (GIBBONS *et al.*, 1975; REIMOLD and STOFFLER, 1978), but the holder in the present case was aluminum and cannot have produced iron particles. On the other hand, there is no need to invoke reduction of Fe^{2+} from the silicates as a source, since the starting material contained Fe-Ni metal phases. Melt veins containing metal and troilite globules are well known in meteorites which have suffered relatively intense natural shock events (RAMDOHR, 1973, p. 58) and it is obvious that the pre-existing metal and troilite were the source of the opaque particles in the experimental veins. Indeed the veins are usually seen to be associated with

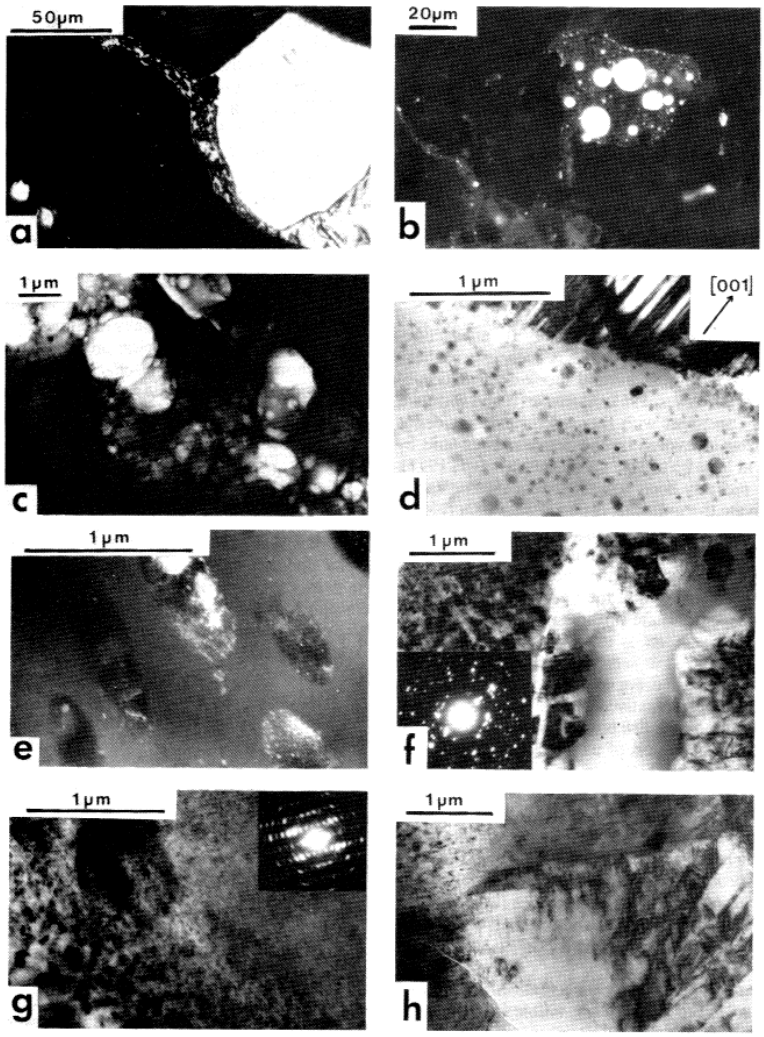

FIG. 5. The spiked-shock sample. (a), (b) reflected light, oil immersion; (c)–(h) HVEM. (a) vein emanating from the boundary of large, primary metal and troilite grains; white is metal, grey troilite, and black silicate. (b) melt pocket containing metal globules. (c) glass vein approximately 5 μm wide among silicate grains. The solids appear dark: The bright, electron-transparent areas are vesicles (gas bubbles) in the vein. (d) the edge of a vein in olivine. The olivine is viewed approximately along [121]. (e) part of another vein, viewed under dark-field conditions. The crystalline blebs were identified as troilite from the diffraction pattern of the strongly diffracting (bright) grain in the upper center. (f)–(h) adjacent areas, viewed in approximately the same orientation, showing effects on olivine of locally concentrated deformation. (f) glass patch and polycrystalline olivine. The inset diffraction pattern is from the left-hand part of the area. (g) immediately to the right of (f); olivine with a spotty appearance giving the mosaicked single-crystal diffraction pattern. (h) the "spotty" material (left) passes into heavily deformed but otherwise normal olivine.

the primary opaque grains within the plane of the section (Fig. 5a). Veins near metal grains usually contain metal globules; those near troilite are usually rich in irregular troilite particles. Many veins have an imperfect polished surface due to the presence of vesicles (see below). The veins closely resemble the narrow black veins in the shock-lithified gas-rich chondrite St. Mesmin (ASHWORTH and BARBER, 1976b, Fig. 3b).

The veins are seen in HVEM to comprise glass with rounded inclusions and, generally, vesicles (Fig. 5c). Figures 5d and 5e show details of introgranular veins in olivine. In Fig. 6d the edge of the deformed olivine is corroded, so some of the vein material was presumably generated *in situ*. The small, rounded inclusions here are present in too small a quantity for identification, but the larger, elongate inclusions in Fig. 5e are identified as troilite. The elongation is parallel to the edge of the vein. There is no crystallographic orientation relation between blebs, and the larger blebs are polycrystalline. The identification of troilite signifies that discrete particles as small as 1 μm have been transported into the vein which now fills a crack in an olivine grain. The shape of the blebs is consistent with origins as droplets of sulphide melt, im-

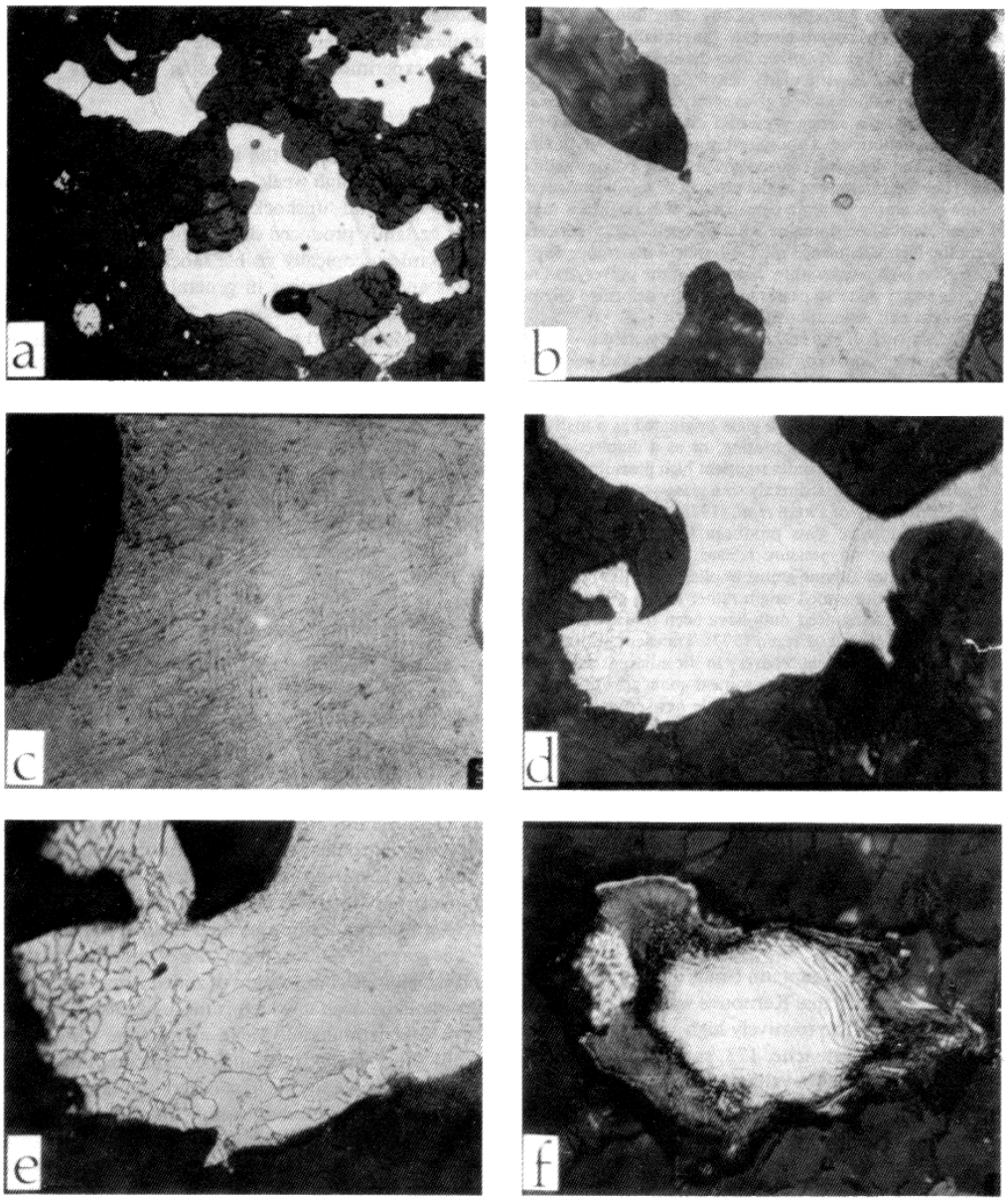

FIG. 6. (a) kamacite with abundant Neumann bands, cracked troilite and silicates in the 270 kbar specimen. Horizontal field of view 1.15 mm. (b) kamacite grain in the 270 kbar specimen showing well-developed shock transformation structure (ϵ-kamacite). Horizontal field of view 115 μm. (c) cross-hatched ϵ-kamacite in the 270 kbar specimen. Note the denser development of grain boundaries. Horizontal field of view 86 μm. (d) a kamacite grain in the spike-shocked specimen. Diffuse ϵ-kamacite is showing incipient recrystallization and α_2 (see Fig. 7c). Horizontal field of view 230 μm. (e) an enlarged region of the grain shown in the previous figure. The α_2 phase has formed by massive transformation of kamacite following heating to >800°C and rapid quenching. Horizontal field of view 90 μm. (f) a zoned taenite (γ) grain in the spike-shocked specimen. The clear γ rim has become disrupted, the cloudy border displays incipient decomposition and the interior shows slip lines. Horizontal field of view 70 μm.

miscible with the silicate melt and elongated in the flow direction. Sulphides crystallize relatively easily from the melt, so the troilite is now crystalline while the host silicate is a glass.

In one olivine grain, a patch of glass with a few vesicles or inclusions is bordered by new, randomly oriented olivine grains up to 1 μm in size (Fig. 5f). Several individual grains were confirmed by electron diffraction to be olivine; no ev-

idence was found for presence of any other mineral. Grains adjacent to the glass are elongate tangentially to the glass interface and have clearly grown from the amorphous material. The host olivine is particularly heavily deformed. Adjacent to the polycrystalline area, it gives spotty contrast from small domains having a strong preferred orientation, giving the diffraction pattern of a mosaiced single crystal of olivine (Fig. 5g). The domains coarsen towards the polycrystalline area. They are interpreted as the product of re-adjustment of olivine containing extreme densities of defects, into a mass of small defect-free domains without open cracks between them; the highly deformed olivine has here undergone slight recovery at high temperature. Away from the polycrystalline area, the spotty material passes into heavily deformed olivine with cracks and dislocations (Fig. 5h).

The glass patch of Fig. 5e, having largely reverted to olivine, must have been close to olivine in composition and was probably generated *in situ* in a region of particularly high strain. In the absence of high-pressure crystalline products, it is difficult to judge whether such a glass originated as a melt due to localized deformational heating, or as a diaplectic glass (JEANLOZ *et al.*, 1977). Under transient high pressures, olivine can probably transform directly to a glass—a prograde glass in the terminology of PRICE *et al.* (1979), as distinct from a retrograde diaplectic glass produced from a high-pressure crystalline phase on pressure release. The nucleation and growth of the new olivine grains implies some thermal effect but does not prove a melt origin rather than a prograde diaplectic one. Heating need only have been transient; olivine growth is rapid (JEANLOZ *et al.*, 1977). Transient heating also accounts for the incipient recovery in the adjacent deformed olivine (Fig. 5g). There has been some domain growth, leading towards the formation of recognizable new crystals (recrystallization in the solid state). Fine-grained areas in the Saint-Severin chondrite (ASHWORTH and BARBER, 1977, Fig. 1c) are attributed to this process, preserving a strong preferred orientation of grains. Nucleation from an amorphous phase, on the other hand, has produced a random orientation of grains in Fig. 5f.

METALLOGRAPHIC OBSERVATIONS

'Unshocked' Kernouve

The presence of Neumann bands in the 'unshocked' meteorite indicates that Kernouve was lightly shocked pre-terrestrially. The relatively high Vickers Hardness Number for the kamacite, 173, supports this conclusion. However, Kernouve is one of the least shocked H-group chondrites that were examined metallographically by HUTCHISON *et al.* (1981).

The 70 kbar shock specimen

The kamacite contains only weak Neumann bands, and it is difficult to establish which belong to the first, pre-terrestrial, generation and which were produced during shock loading. Other than some mild plastic deformation of metal grains which occurs near the periphery, there has been little or no gross deformation of metal grains in the sample. HV_α is quite high (mean of 11 measurements was 229 ± 17) and there is a noticeable decrease in hardness of kamacite grains from the edge (~266) to the center (~210) of the specimen well away from the encasing material. There are no microscopically visible shock effects in taenite, and grains are generally too small to obtain a reliable VHN.

Under crossed polars troilite shows undulose extinction and weak shock twins which are absent in the 'unshocked' material and were certainly produced during experimental shock loading.

The 165 kbar shock specimen

Neumann bands in the kamacite of the 165 kbar specimen, although weak, are more abundant than in the 70 kbar and 'unshocked' samples; some were almost certainly produced during shock loading. There are no microscopically visible shock effects in taenite grains and metal grains in general do not show any gross deformation.

HV_α (mean of 10 measurements is 256) is high, as is our one measurement of HV_γ (~414), and reflects shock-hardening. However, only localized, incipient ϵ kamacite was observed and kamacite has not undergone a general polymorphic transformation to ϵ kamacite. Troilite displays abundant shock twins and some small scale (10–20 μm) incipient polycrystallinity at the margins of grains. As in the 70 kbar specimen there is a decrease in HV_α from rim to core of the fragment.

The 390 kbar shock specimen

Kamacite contains abundant deformation bands and displays ϵ-kamacite transformation which is diffuse and indistinct notably at grain boundaries. There has been overall deformation of metal grains which are irregular and ragged. HV_α 359 ± 18 is lower than that for the spike-shocked and 270 kbar specimens. Very few taenite grains are present in the sample and it was not possible to obtain a hardness measurement. Taenite grains in general do not show extensive shock alterations but some grains do display rare slip lines and incipient decomposition of their cloudy borders.

The generally diffuse appearance of epsilon-kamacite and incipient decomposition of zoned taenite, indicate post-shock annealing which is more extensive than in the 270 kbar material. Metal and troilite have been locally shock-melted, although eutectic melting is not extensive. Unlike the spike-shocked sample, however, kamacite in the 390 kbar sample does not display α_2 transformations. The metallographic features indicate brief ambient relaxation temperature in the range 500–600°C, intermediate to the 270 and spike-shocked specimens.

Troilite is badly cracked and fissured displaying shock-twins and localized small scale polycrystallinity.

The 270 kbar shock specimen

The sample examined metallographically consists of three small fragments potted in araldite. Metal grains have ragged outlines, particularly those occurring near the edges of the fragments. However, there has not been extensive gross deformation of metal grains. Kamacite displays abundant Neumann bands (Fig. 6a) and well developed cross-hatched ϵ-kamacite (Figs. 6b and 6c). There is a noticeable increase in the density of the cross-hatching at kamacite/silicate grain bound-

aries, and some kamacite grains show localized incipient shear deformation.

The hardness of kamacite is very high (367 ± 27) and reflects the shock-hardened ϵ-kamacite. No shock effects were observed in γ (taenite) grains at the resolution of the optical microscope, but its hardness (average of 2 measurements is ~460) was the highest measured in any of the shocked samples. No unambiguous shock reheating effects were observed in either kamacite or taenite phases. However, patches of diffuse and indistinct ϵ-kamacite along the grain boundaries of some kamacite grains could indicate the onset of recrystallization. The very high HV_α figure indicates that any annealing was very short lived and localized.

Troilite is badly cracked, displays undulose extinction under cross polars and contains abundant shock twins. Along grain boundaries there is some small scale (up to 20 μm units) polycrystallinity which is more abundant and better developed than that observed in the 165 kbar sample. Locally troilite has been compressed sufficiently to produce incipient melting and there is some veining of the surrounding silicates which are heavily cracked and brecciated. Sulphide/metal interfaces have remained intact and there is no evidence of eutectic melting.

The specimen subjected to a spiked-shock pulse

This sample displayed the greatest range of shock-induced effects. Throughout the bulk of the sample gross deformation of metal grains is extensive. Silicate grains have been kneaded into metal grains (see Fig. 6d) causing localized small-scale shear deformation and giving a generally ragged appearance to the metal. Kamacite displays abundant deformation bands and diffuse cross-hatched ϵ-kamacite. Epsilon-kamacite along interfaces with silicate in some large kamacite grains has been locally transformed to α_2 and some small (<100 μm) kamacite grains show complete transformations. Fine grained recrystallization has also occurred along sheared surfaces in kamacite grains (see Figs. 6d and 6e).

The generally diffuse and mottled appearance of ϵ-kamacite in the bulk of grains, and localized α_2 transformations are clear indications of widespread shock-annealing reheating and incipient recrystallization. There is also evidence along kamacite grain boundaries of oxidation at elevated temperatures. The mean HV_α of 9 'core' measurements (361 ± 14) is lower than the hardness of kamacite in the 270 kbar specimen and reflects the softening which accompanies annealing and recovery. One measurement HV_α was as low as 152, which indicates complete recovery.

Unfortunately, taenite grains were too small to obtain meaningful hardness measurements. However, zoned taenite grains also display gross deformation. Often their clear rims have been disrupted due to pressure from the surrounding silicates. Where severe surface deformation has occurred, zoned taenite grains contain parallel arrays of slip lines (Fig. 6f). Many zoned taenite grains show the effects of annealing by the incipient decomposition and reticulation of their cloudy borders (Fig. 6f).

Troilite, metal and silicates have been extensively mobilized and there is abundant veining of the badly cracked silicates. Unmelted troilite is strongly polycrystalline consisting of fine grained 50 μm units. Throughout the specimen metal and sulphide occur in the numerous 'melt pockets' (see Figs. 5a, b).

From the observed metallic microstructures it is possible to establish rough limits for the ambient relaxation temperature after shock. Epsilon-kamacite when heated for a short time in the laboratory to temperatures below 450°C does not recrystallize (JAIN and LIPSCHUTZ, 1968; BRENTALL and AXON, 1962). Since there has been extensive annealing of ϵ-kamacite we can set a lower limit for the ambient relaxation temperature at around 500–600°C. Kamacite, whether deformed or not, when heated above 750°C into the γ-region of the Fe-Ni system will, on rapid cooling, martensitically transform to the distorted α_2 structure. In the 335 kbar specimen α_2 occurs locally, particularly where kamacite grains abut 'melt pockets'. However, only a small proportion of the grains have been transformed to α_2 and an upper limit for the ambient relaxation temperature is therefore set at about 800°C.

Locally much higher temperatures must have been attained during shock to produce melted metal, troilite and silicate. Reflection and attenuation of the shock wave at grain boundaries produced localized melting where temperatures rose to around 1000°C. However, the ambient temperature must briefly have been of the order of 600–800°C.

Microhardness measurements

The mean hardness measurements for kamacite and taenite in the five shocked and one natural Kernouve sample are summarized in Fig. 7. The most noteworthy point is that the $\alpha \rightarrow \epsilon$ transformation for kamacite in Kernouve appears to lie between 163 and 270 kbar. This is 30–40 kbar, or more, higher than that observed by BUCHWALD (1975) in experimentally shocked Odessa iron meteorite. The difference would seem to be related to the ability of the silicates and, more especially, troilite to act as shock-absorbers, a possibility invoked by HEYMANN (1967) to explain why ϵ-kamacite is not commonly found in chondrites. Another factor which could change the transformation pressure is composition (ZUKAS, 1969), but since there is good overlap in Ni compositions of chondritic metal and iron meteorites this is unlikely to be significant.

Despite the difference in $\alpha - \epsilon$ transformation pressure the present data are in good agreement with BUCHWALD's (1975) data. There is a moderate increase in hardness of the kamacite up to the $\alpha - \epsilon$ transformation which is accompanied by a sharp increase in hardness to around 360. At higher shock pressures there is a gradual decrease in hardness. There is much evidence in the spike-shocked specimen that the de-

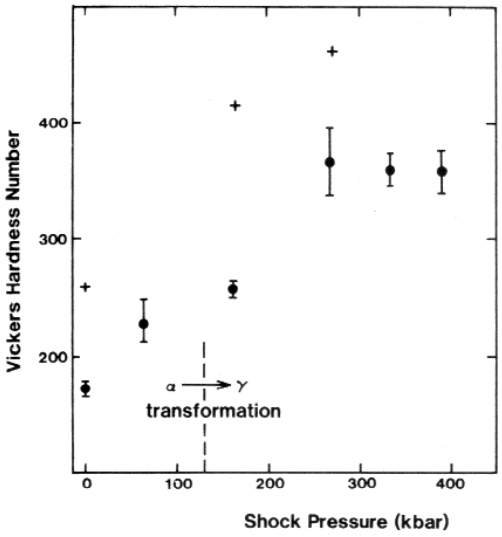

FIG. 7. Vickers Hardness Number for kamacite and taenite as a function of shock intensity experienced. The hardness of the kamacite increases steadily with increasing pressure, but levels off in the samples in which the shock transformation structure observed. The apparent $\alpha \rightarrow \epsilon$ transformation pressure is around 200 kbar, somewhat higher than observed for iron meteorites (see text). Taenite data are few because of its small grain size, but show a steady increase with shock pressure.

crease results from shock-annealing and incipient recrystallization of ϵ-kamacite. The 390 kbar data could be spurious, since only minor annealing effects were observed in the sample and the lower hardness is, rather, due to the different shock history of the specimen given a spiked pulse.

Although based on few data points, the hardness of the taenite shows a steady increase over a wide range of pressures.

THERMOLUMINESCENCE RESULTS

Our data are presented in Table 2 and Figs. 8 and 9. Neither of the two shock experiments below 200 kbar produced any measureable changes in the TL properties of the meteorite samples. At shock pressures in excess of 200 kbar, there was a substantial decrease in both the natural TL and the amount of TL which can be induced by a standard laboratory radiation dose on a drained sample. The decrease in the intensity of the low temperature peak showed the most spectacular effect, dropping by a factor of 10^{-2} in the 270 kbar sample and 10^{-3} in the 390 kbar sample. The decrease shown by the high temperature TL was much less, the 270 kbar sample being lower than the unshocked material by a factor of 10^{-1} and the TL of the 390 kbar sample was lower than the natural sample by $\sim 15^{-1}$. Apparently, either the low temperature TL is more sensitive to shock or some thermal annealing occurs at pressures above 200 kbar.

The decrease in the amount of TL which can be induced in the shocked samples as pressures increased is not so marked. Samples shocked to >200 kbar have TL sensitivities which are lower than unshocked material by a factor of <10. Unlike the changes in natural TL, the behavior of the TL in the high and low temperature regions is very similar. Clearly the effect of shock on the TL properties of meteorites involves more than simple thermal drainage of electron traps. We can remove the effect of changes in the TL phosphor, and examine only the effect of thermal draining, by considering the ratio of the natural TL to the induced TL (Fig. 10). Below 200 kbar, there appears to have been no thermal drainage in either the low temperature or high temperature regions of the glow curve. Above 200 kbar, the low temperature TL drops steadily by up to nearly two orders of magnitude. The high temperature TL drops by about 50% between the 165 and 270 kbar samples and thereafter shows no dependence on shock pressure. Apparently, all samples shocked to >200 kbar suffered thermal drainage to all regions of the glow curve, but only in the low temperature region was it systematically related to pressure.

There are apparently two kinds of processes occurring in the TL of these samples as a result of the high shock levels experienced. One process is reversible in that it may be restored by artificially irradiating the sample. This effect is strongest in the lower temperature regions of glow curves and is presumably thermal drainage. The second process results in permanent changes to the sample which is not reversed by the 50 krad radiation dose administered in the laboratory. It seems to have affected all regions of the glow curve equally and is presumably associated with permanent changes in the phosphor.

In the equilibrated St. Severin meteorite, the TL phosphor is known to be located in the low-density, feldspar-rich fraction (LALOU *et al.*, 1971). Since feldspar is highly sensitive to the levels of shock and reheating involved in these experiments, the most plau-

Table 2. Thermoluminescence data on artificially shock loaded Kernouve meteorite.

Shock Pressure (kbar)	Thermoluminescence* Natural TL	mean	TL Sensitivity	mean
Natural	0.90	1.0	1.13	1.0
	1.10		0.87	
70	0.92	0.85	0.64	0.64
	0.77		0.64	
165	0.79	0.88	0.92	0.98
	0.97		1.03	
270	0.011	0.011	0.091	0.088
	0.011		0.085	
390	0.0011	0.0011	0.033	0.033
	0.0011		0.033	
Spike-shocked+	0.0017	0.0016	0.0026	0.0029
	0.0015		0.0031	

* Where natural Kernouve = 1. The values refer to the height of the low temperature peak height.

\+ This specimen was shock loaded under different conditions to the others to an ill-determined pressure (see text).

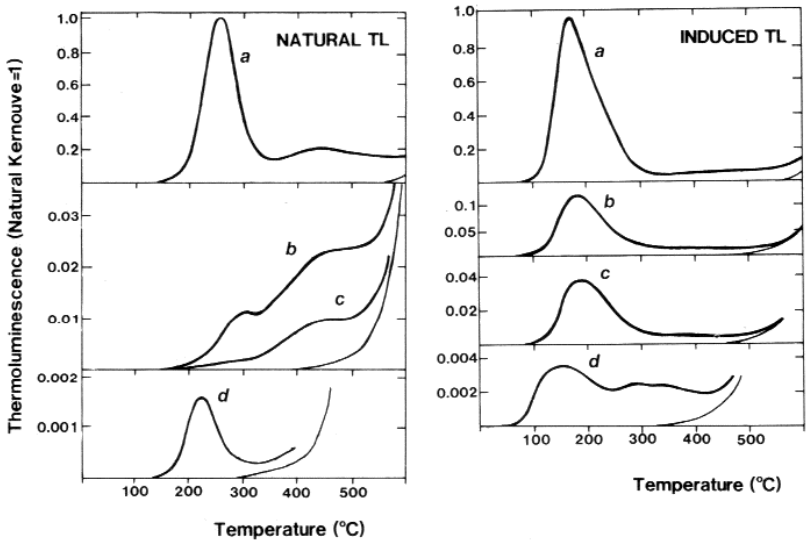

FIG. 8. Glow curves (thermoluminescence against temperature) for samples of the Kernouve meteorite subjected to shock: (a) natural. (b) 270 kbar. (c) 390 kbar. (d) shock pulse with a "spiked" profile, of unknown but high intensity. The curves for the 70 and 165 kbar samples resemble those of the unshocked material. The low temperature TL seems to be removed more effectively than the high temperature in the more heavily shocked material. The exception is the spike-shocked sample, for which the high temperature TL seems to have been less stable. The curve on the right for each plot is the background black-body radiation. On the right, glow curves for the TL displayed after the samples have had their natural TL drained by heating to 500° and then given a standard test dose of radiation. Unlike natural TL curves on the left, in the low temperature peak always dominates, but again the spike-shock specimen shows behavior unlike the others.

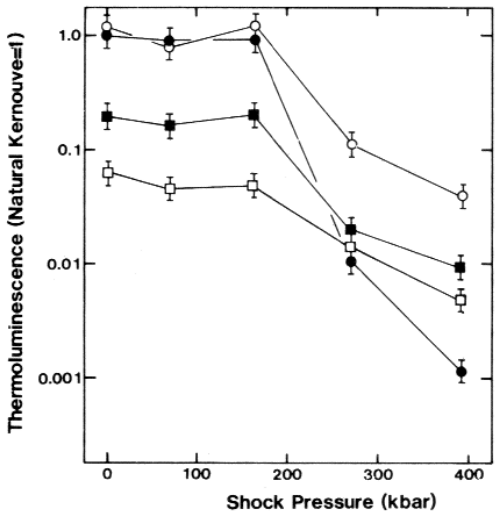

FIG. 9. Thermoluminescence *vs.* shock pressure. Filled symbols: Natural thermoluminescence in the low temperature (circles) and high temperature (squares) regions of the glow curves (see Fig. 8). Above ~200 kbar, the low temperature TL falls systematically with shock, but the high temperature TL seems to have been particularly affected in the case of the spike-shocked experiment. Open symbols: TL induced in a drained sample by a standard radiation dose. As with natural TL, shocks greater than ~200 kbar cause a decrease in TL sensitivity but the effect is not so marked. Data for the spike-shocked sample (see Table 2) are not plotted.

sible interpretation of the TL data is that the phosphor is feldspar and that shock-induced changes in the feldspar are having a strong influence on the TL properties.

Figure 8 shows representative glow curves for the natural TL and induced TL of the present samples. The differences in the temperature and width of the low temperature peak in the natural and induced TL curves is due to thermal drainage of the low temperature TL in the natural samples. In the induced curves there is a slight tendency for the low temperature peak to move to higher temperatures and broaden as the TL intensity decreases. If the TL peak were due to a single trap this would be interpreted as indicating second order kinetics for the TL mechanism, but since the "peak" is known to consist of several separate peaks an alternative explanation is that lower temperature traps are preferentially being destroyed.

LIENER (1966) and LIENER and GEISS (1968) have measured the natural TL and the TL sensitivity of artificially shock loaded material from the Stalldalen chondrite (FREDRIKSSON *et al.*, 1963). A sample shock loaded to 150–300 kbar had natural TL which was only 4.8% of the unshocked value, whereas its TL sensitivity was 93%. A sample shocked to 500–800 kbar had both its natural TL and TL sensitivity appreciably lowered, to 2.7% and 9.3%, respectively. Apparently the natural TL in these experiments was less stable than the TL sensitivity, again suggesting that thermal draining was occurring as well as more fun-

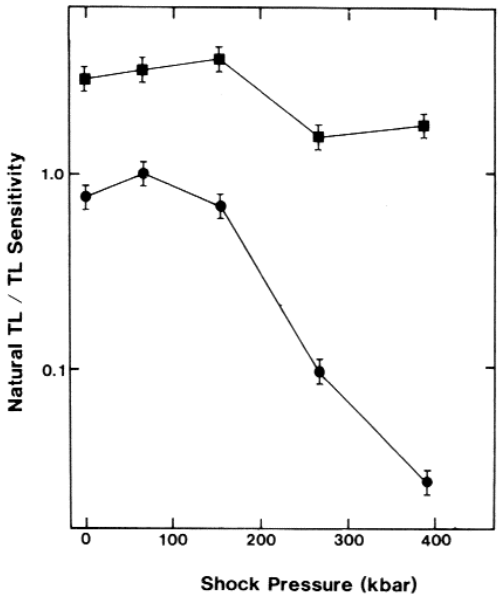

FIG. 10. A plot of natural thermoluminescence normalized to TL sensitivity as a function of shock pressure. It is apparent that the high temperature TL in the natural samples as well as the low temperature TL has been drained by the shock event. (Circles, low temperature TL; squares, high temperature TL).

damental changes in the phosphor. The agreement between Liener's and the present data is quantitatively good, if one assumes that the sample in Liener's lower pressure range was actually shocked to values near the upper limit of that range.

The sample subjected to a spiked shock pulse

This sample has considerably lower TL than any other sample; in the low temperature region of the glow curve both natural TL and TL sensitivity are lower than in unshocked material by nearly three orders of magnitude. The TL data therefore suggest that this was the most strongly shocked sample. The especially low TL levels are consistent with the idea that the TL properties of these samples reflect changes in the feldspar because of the thorough maskelynitization of plagioclase noted in this sample.

Besides its especially low TL, this sample differs from the other samples in the shape of the glow curves it produces. The glow curve for the natural TL is noteworthy in having a pronounced low temperature peak, whereas the glow curve for the induced TL has a low temperature peak comparable in intensity to the high temperature TL. Such a situation might imply that the intense shock did not simply destroy traps, but also repopulated some of the low temperature traps. However the temperature of the low temperature peak is somewhat lower than in less-shocked samples suggesting not merely re-population of existing traps but the creation of a new kind of trap. This could reflect the production of a new phase or mineral, but we have not detected a new crystalline phase that could be a phosphor. The effect may be a modification in the remaining plagioclase, a pressure-induced thermoluminescence comparable to that discussed by ANGINO (1964). The mechanism of the effect is obscure. It is noteworthy that other physical properties of plagioclase, such as lattice parameters, are noticeably affected by shock-loading (SCHNEIDER, 1977). The new traps apparently have a much lower TL sensitivity compared with the other specimens, but their natural TL is much more stable to the shock experienced.

DISCUSSION

Range of pressures considered here compared with the naturally observed range

Metallographic studies of naturally shocked meteorites indicate that the range of pressures we have achieved is probably less than those naturally experienced. According to the studies of HEYMANN (1967), WOOD (1967), TAYLOR and HEYMANN (1969, 1970, 1971), BEGEMANN and WLOTZKA (1969) and SMITH and GOLDSTEIN (1977) increasing levels of shock produce the following metallographic changes to the primary cooling features of opaque minerals in chondrites: *lightly shocked*—monocrystalline kamacite containing Neumann bands, whereas zoned taenite and normal plessite remain unaltered (*e.g.*, Kernouve); *moderately shocked*—recrystallized kamacite (α_2), normal zoned taenite and plessite (*e.g.*, Bruderheim); *moderately to strongly shocked*—recrystallized kamacite, no zoned taenite or plessite, melted troilite (*e.g.*, Ergheo); *heavily shocked*—clear polycrystalline kamacite and troilite which has melted and become polyphase at the periphery (*e.g.*, McKinney and Kingfisher); *very heavily shocked*—clear polycrystalline kamacite, Ni-rich martensite and large ovoid metal-sulfide structures (*e.g.*, Farmington and Lubbock). The latter also contain >0.1 at % P in the kamacite, phosphides, very large Ni-gradients in the metal and precipitates of secondary kamacite. A detailed comparison of the present data and naturally shocked chondrites has not yet been made, but several pertinent remarks are possible on the basis of these literature generalizations. Troilite has melted in moderate to strongly shocked meteorites so presumably our 270 kbar sample, in which there is only incipient melting but many shock effects, is broadly analogous to the moderately shocked natural meteorites. Many of the effects observed in the spike-shocked specimen resemble the heavily shocked natural samples; in addition to shock blackening there is polycrystalline kamacite, extensive sulfide mobilization and decomposition of taenite. However, we do not observe Ni-rich martensite or large ovoid metal-sulfide structures. Our studies revealed a large range of shock induced changes in the troilite—twins, polycrystallinity, undulose extinction, partial and complete melting and metal-sulfide eutectic melts—many of which have yet to be described in naturally shocked specimens.

Our data for the silicates also leads to the conclusion, that we did not achieve the range pressures that have occurred naturally. Our experiments did produce the very high pressures which would induce optically visible recrystallization in olivine (CARTER *et al.*, 1968; REIMOLD and STOFFLER, 1978) or new crystalline silicate phases (PRICE *et al.*, 1979). On the other hand, none of the pressures produced in the present case were mild enough to inhibit (001) twinning in diopside (*cf.* ASHWORTH, 1980b).

The TL of 12 naturally shocked ordinary chondrites was examined by SEARS (1980). According to various types of literature data he reviewed, mainly metallographic and XRD studies of olivine, black chondrites have typically suffered shock waves of a few hundred kbar to 1 Mbar. Their natural TL and their TL sensitivity were much lower than unshocked meteorites of the same classes by factors of 10^{-1} to 10^{-2}. The natural TL of 14 meteorites with a variety of shock histories is plotted against TL sensitivity in Fig. 11. Each meteorite has been assigned a "ranking order" reflecting the degree of shock/reheating it has experienced, 1 indicates little or none, 8 indicates the most heavily shocked samples (see the Appendix in SEARS, 1980, for details). With the exception of Olivenza and Wickenberg, the chondrites lie within a factor of 2–3 of the unity line indicating that the natural TL to TL sensitivity ratio for the shocked meteorites is comparable with that for the unshocked meteorites. Apparently the lower levels of natural TL observed in shocked chondrites is attributable entirely to their lower TL sensitivity (*i.e.*, they have suffered similar histories of exposure to ionizing radiations and elevated temperatures). It is possible to conclude that the shock event which lowered the TL sensitivity of certain meteorites occurred a sufficiently long time ago, probably about 500 my ago (TURNER *et al.*, 1978), that the TL has had time to return to equilibrium. The explanation for the two meteorites which lie below the diagonal (Olivenza and Wickenburg) is not straightforward. Perhaps they were shocked recently and their TL has not had long enough to return to its equilibrium level, but Olivenza had received very little shock compared to the others and was given a 1 ranking. Other factors which could be responsible for low natural TL are a recent heating, such as a close solar passage or artificial heating, a large terrestrial age (not applicable to Olivenza) or a different cosmic ray exposure history, such as different shielding or orbits (see MCKEEVER and SEARS, 1980, for a review).

Unlike natural TL, the TL sensitivity changes seem to be permanent. Experiments aimed at increasing the TL sensitivity by radiation damage were performed by SEARS (1980). Samples of the Kernouve meteorite were exposed to doses of α, β, γ radiation and protons comparable or greater than the dose thought to have been experienced by the meteorite over its entire lifespan, but no increase in TL sensitivity was observed within experimental limits. It seems therefore that TL sensitivity may be used as a reliable indicator of the shock history of meteorites, independent of the radiation history and all but the most prolonged heating episodes. Thus, we believe that the meteorites with a shock ranking of 5–8 have received shock impulses in the range of 270–390, that those with a ranking of 1 have probably received pressure < 270 while none of the samples plotted in Fig. 11 have apparently been shocked as severely as our "spike-shock" sample.

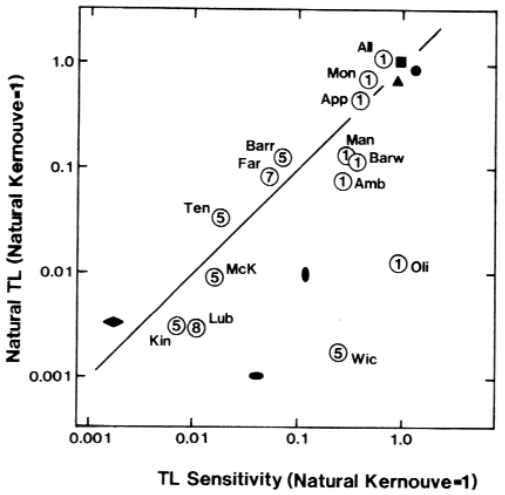

FIG. 11. An attempt to compare the present data on artificially shock loaded meteorite material with the TL of 14 ordinary chondrites with a variety of shock histories. 0 kbar ●, 70 kbar ▲, 165 kbar ■, 270 kbar ⬮, 390 kbar ⬬, spike shock ◆. Data from the low temperature region of the glow curve are used. Most naturally shocked meteorites lie on or near the unity line indicating that their natural TL has returned to equilibrium after the shock; in contrast the 270 and 390 kbar artificially shocked samples have a much reduced natural TL. The spike-shocked sample lies near the unity line, suggesting that the natural TL was not drained by the shock but its low value is entirely attributable to low TL sensitivity. This is consistent with a new shock insensitive mineral becoming the dominant phosphor, or with the shock repopulating the traps in the LT region of the glow curve.

Thermal effects

The metallographic results enable post-shock temperatures to be estimated. In the 390 kbar sample, a fairly widespread annealing to 400–500°C seems to have occurred. In the spike-shocked specimen there is much evidence of widespread annealing of the opaque minerals to, perhaps, 600–800°C. The annealing was too transient for modification (recovery) of the deformational substructures in silicates, except perhaps very locally (Fig. 5g). We never observed polycrystalline kamacite, although this is present in moderately shocked natural specimens. Presumably our samples were too small to suffer the widespread post-shock annealing that comparably shocked natural specimens received. Thus it is not surprising that the TL effects are more comparable with the naturally shocked meteorites than are the metallographic results.

Transient heating is sufficient to explain the thermal emptying of TL traps. The shock-related metallographic effects discussed in the literature are nearly all really reheating effects requiring a finite annealing period (TAYLOR and HEYMANN, 1969). The cooling rate following the artificial shock will almost certainly be much faster than that following the natural shock. Efficient quenching is also indicated by the glassy state of the silicate melt veins in the spike-shocked sample: very similar, natural veins in the shock-lithified gas-rich chondrite St. Mesmin are microcrystalline rather than glassy (ASHWORTH and BARBER, 1976b, Fig. 3c), indicating less rapid cooling or subsequent slight heating.

Effects of very high temperatures (melting) are localized at grain boundaries. It is noteworthy that although very local melting is inferred even in the 165 kbar sample (Fig. 4g), it does not seem to have been widespread enough to heat the sample sufficiently to drain the natural TL (~200°C). The different experimental conditions experienced by the spike-shocked sample, while not noticeably affecting deformation mechanisms within crystals, must have contributed to the veining-lithification effect in the bulk rock. Whereas the 390 kbar sample was disrupted by the experiment, in the spike-shocked sample many fractures became sealed by injected melt before disintegration could occur. The result is very like a shock-lithified breccia (*cf.* ASHWORTH and BARBER, 1976b), with the difference that in the Kernouve material fragmentation occurred immediately before lithification, during the experiment. This catastrophic fragmentation was accompanied by intense internal deformation throughout the grains, whereas many grains in the shock-lithified gas-rich meteorites are internally undeformed (ASHWORTH and BARBER, 1976b). Acting on media that were already very porous, the shocks required for lithification were presumably rather mild.

Variations in deformation effects with shock pressure

The experiments extended to more severe conditions than those responsible for the features previously studied in naturally shocked meteoritic olivine (ASHWORTH and BARBER, 1975) and pyroxene (ASHWORTH and BARBER, 1976a). In olivine, dislocation density increases with increasing peak pressure. The etching study confirms that initially (at low peak pressure) dislocations are generated on slip planes that are distinguishable from preexisting subgrain boundaries. Only above 165 kbar were dislocations pervasively distributed throughout large olivine grains. This development, together with increased cracking, correlates with the onset of optical mosaicism. The data are consistent with the optical observation, in chondrites showing heavy natural shock-deformation, that optical mosaicism of olivine develops under conditions slightly less severe than those required for conversion of most of the plagioclase to maskelynite (DODD and JAROSEWICH, 1979). The results are also consistent with the experimentally determined peak pressure of 220 kbar for the onset of optical mosaicism in polycrystalline olivine (BAUER, 1979).

In plagioclase, the main effect is progressive conversion to maskelynite. The finding of some crystalline plagioclase in the 270 kbar specimen is consistent with the TL sensitivity data, since the TL in the specimen shocked to 390 kbar is a factor of ~50 lower than those shocked to <200 kbar, while the 270 kbar specimen is intermediate in its TL sensitivity. Setting aside the spike-shocked sample, we argued earlier that our TL data can be interpreted in terms of two processes, one which emptied traps and one which destroyed traps. The former process has been identified as thermal. We can now identify the latter process as primarily the inversion of plagioclase to maskelynite. However, effects more subtle than vitrification may also play a part in determining TL sensitivity, since the crystal structure of plagioclase is known to be affected by shock: the lattice expands, probably during pressure release (SCHNEIDER, 1977). We speculate that in the spike-shocked experiment this modified plagioclase became the dominant phosphor. Whether this would yield TL properties of the kind observed is currently a matter of conjecture.

In orthopyroxene, the development of clino-lamellae at 66 kbar is closely comparable to that in natural specimens (ASHWORTH and BARBER, 1976a). The prevalence of the unit-dislocation mechanism at higher pressures is an important observation. It means that ASHWORTH (1979b) was wrong to suggest that this mechanism indicates high ambient temperatures at the time of deformation. Moreover, great care must be exercised in attempting to distinguish deformation by this mechanism from post-deformational recovery of orthopyroxene containing clino-lamellae; elimination of clino-lamellae during annealing is itself accompanied by the introduction of unit dislocations (COE and KIRBY, 1975). There may be some future in the argument that broad clino-lamellae are preferentially retained during the latter process (ASHWORTH, 1980a). Recovered dislocation distributions in olivine (ASHWORTH and BARBER, 1977; ASHWORTH, 1979b, 1981) are probably a safer guide to thermal history, since nothing like them was observed in the present study. Meanwhile, clear examples of unit-dislocation slip in orthopyroxene should be sought in naturally shocked meteorites.

For orthopyroxene, the pressure at which the deformation mechanism switches is lower (between 70 and 165 kbar) in the chondrite than the 250–350 kbar estimated in the basaltic rock (NORD and MCGEE, 1979). In metal, on the other hand, the pressure for the $\alpha \rightarrow \epsilon$ transition is at least 30 kbar higher than that determined experimentally in an iron meteorite (BUCHWALD, 1975). Both differences are probably due to the rock-type. This is clear in the case of the metal, whose silicate-sulphide surroundings in chondrites differ fundamentally from the environment in an iron

meteorite. The phase transformation tends to be suppressed by the shock-absorbing effect of the chondrite matrix, particularly the sulphide.

Acknowledgments—We are grateful to Dr. M. H. Loretto (Birmingham University) for the use of the high-voltage electron microscope, Dr. S. Murphy (Department of Metallurgy and Materials, Aston) for SEM facilities, Professor D. J. Barber for instructive discussions, Dr. R. Hutchison (British Museum, Natural History), for supplying the Kernouve material necessary for this study and Mr. K. D. Burrows and Mr. R. L. Gyton (Atomic Weapons Research Establishment, Foulness, Essex) for performing the shock loading experiments and for supplying us with a description of the procedure. This work was supported by the Natural Environment Research Council (JRA) and by the Science and Engineering Research Council, National Aeronautics and Space Administration and the Research Corporation (DWS).

REFERENCES

ANGINO E. E. (1964) The effects of non-hydrostatic pressures on radiation-damage thermoluminescence. *Geochim. Cosmochim. Acta* **28,** 381–388.

ASHWORTH J. R. (1979a) Two kinds of exsolution in chondritic olivine. *Mineralog. Mag.* **43,** 535–538.

ASHWORTH J. R. (1979b) Electron microscope observations bearing on the early histories of ordinary chondrites (abstract). *Meteoritics* **14,** 338–339.

ASHWORTH J. R. (1980a) Chondrite thermal histories: Clues from electron microscopy of orthopyroxene. *Earth Planet. Sci. Lett.* **46,** 167–177.

ASHWORTH J. R. (1980b) Deformation mechanisms in mildly shocked chondritic diopside. *Meteoritics* **15,** 105–115.

ASHWORTH J. R. (1981) Fine structure in H-group chondrites. *Proc. Roy. Soc. Lond.* **A374,** 179–194.

ASHWORTH J. R. and BARBER D. J. (1975) Electron petrography of shock-deformed olivine in stony meteorites. *Earth Planet. Sci. Lett.* **27,** 43–50.

ASHWORTH J. R. and BARBER D. J. (1976a) Shock effects in meteoritic pyroxene. In *Developments in Electron Microscopy and Analysis* (ed. J. A. VENABLES), pp. 517–520. Academic Press, London.

ASHWORTH J. R. and BARBER D. J. (1976b) Lithification of gas-rich meteorites. *Earth Planet. Sci. Lett.* **30,** 222–233.

ASHWORTH J. R. and BARBER D. J. (1977) Electron microscopy of some stony meteorites. *Phil. Trans. Roy. Soc. Lond.* **A286,** 493–506.

AVE LALLEMANT H. G. and CARTER N. L. (1972) Deformation of silicates in some Fra Mauro breccias. *Proc. Lunar Sci. Conf. 3rd* **1,** 895–906.

BAUER J. F. (1979) Experimental shock deformation of mono- and polycrystalline olivine: A comparative study. *Proc. Lunar Planet. Sci. Conf. 10th* **3,** 2573–2596.

BEGEMANN F. and WLOTZKA F. A. (1969) Shock-induced thermal metamorphism and mechanical deformations in the Ramsdorf chondrite. *Geochim. Cosmochim. Acta* **33,** 1351–1370.

BOGARD D. D., HUSAIN L. and WRIGHT R. J. (1976) ^{40}Ar-^{39}Ar dating of collisional events in chondrite parent bodies. *J. Geophys. Res.* **81,** 5664–5678.

BRENTNALL W. D. and AXON H. J. (1962) The response of Canyon Diablo meteorite to heat treatment. *Nature* **200,** 947–955.

BUCHWALD V. F. (1975) *Handbook of Iron Meteorites,* University of California Press, Berkeley.

CARTER N. L., RALEIGH C. B. and DECARLI S. (1968) Deformation of olivine in stony meteorites. *J. Geophys. Res.* **73,** 5439–5461.

CHRISTOPHE MICHEL-LEVY M. (1978) Estimation de la porosite de quelques chondrites par analyse d'images de leurs sections polies. *Meteoritics* **13,** 305–309.

CHRISTOPHE MICHEL-LEVY M. (1979) La pierre de Sena: des informations sur les conditions de formation de chondrites a bronzite. *Bull. Mineral.* **102,** 410–414.

COE R. S. and KIRBY S. H. (1975) The orthoenstatite to clinoenstatite transformation by shearing and reversion by annealing: Mechanism and potential applications. *Contrib. Mineral. Petrol.* **52,** 29–55.

DODD R. T. (1969) Metamorphism of ordinary chondrites. *Geochim. Cosmochim. Acta* **33,** 161–203.

DODD R. T. and JAROSEWICH E. (1979) Incipient melting in and shock classification of L-group chondrites. *Earth Planet. Sci. Lett.* **44,** 335–340.

FREDRIKSSON K., DECARLI P. S. and AARAMAE A. (1963) Shock-induced veins in chondrites. *Space Research III,* Proc. 3rd International Space Sci. Symposium, Washington 1962. (ed. W. PRIESTER), 974–983.

GIBBONS R. V. and AHRENS T. J. (1977) Effects of shock processes on calcic plagioclase. *Phys. Chem. Minerals* **1,** 25–107.

GIBBONS R. V., MORRIS R. V., HORZ F. and THOMPSON T. D. (1975) Petrographic and ferromagnetic resonance studies of experimentally shocked regolith analogs. *Proc. Lunar Sci. Conf. 6th* **3,** 3143–3171.

HANSS R. E., MONTAGUE B. R., DAVIS M. K., GALINDO C. and HORZ F. (1978) X-ray diffractometer studies of shocked materials. *Proc. Lunar Planet. Sci. Conf. 9th* **2,** 2773–2787.

HEYMANN D. (1967) On the origin of hypersthene chondrites: Ages and shock effects of black chondrites. *Icarus* **6,** 189–221.

HORZ F. and QUAIDE W. L. (1972) Debye-Scherrer investigations of experimentally shocked silicates. *Moon* **6,** 45–82.

HUSS G. R. (1980) Heterogeneous shock effects in type 3 ordinary chondrites. *Meteoritics* **15,** 305–306.

HUSS G. R., KEIL K. and TAYLOR G. J. (1981) The matrices of unequilibrated ordinary chondrites: Implications for the origin and history of chondrites. *Geochim. Cosmochim. Acta* **45,** 33–51.

HUTCHISON R., BEVAN A. W. R., EASTON A. J. and AGRELL S. O. (1981) Mineral chemistry and genetic relations among H group chondrites. *Proc. Roy. Soc. Lond.* **A374,** 159–178.

JAIN A. V. and LIPSCHUTZ M. E. (1968) Response of previously shocked iron meteorites to heat treatment. *Nature* **220,** 139–143.

JEANLOZ R., AHRENS T. J., LALLY J. S., NORD G. L., JR., CHRISTIE J. M. and HEUER A. H. (1977) Shock-produced olivine glass: First observation. *Science* **197,** 457–459.

KIEFFER S. W., PHAKEY P. P. and CHRISTIE J. M. (1976) Shock processes in porous quartzite: transmission electron microscope observations and theory. *Contrib. Mineral. Petrol.* **59,** 41–93.

LALOU C., BRITO U., NORDEMANN D. and MARY M. (1970) TL induite dans des cibles epaises par des protons de 3 GeV. *C.r. hebd. Seance. Acad. Sci. (Paris) Serie D* **270,** 1706–1708.

LIENER A. (1966) Thermolumineszenzmessungen an Meteoriten. Ph.D. Thesis, University of Berne, 1–45.

LIENER A. and GEISS J. (1968) Thermoluminescence measurements on chondritic meteorites. In *Thermoluminescence of Geological Materials* (ed. D. J. MCDOUGALL), pp. 559–578. Academic Press, New York.

MCKEEVER S. W. S. and SEARS D. W. (1980) Natural thermoluminescence of meteorites—A pointer to orbits? *Modern Geology* **7,** 137–145.

MILLS A. A., SEARS D. W. and HEARSEY R. (1977) Apparatus for the measurement of thermoluminescence. *J. Phys. (E)* **10,** 51–56.

NORD G. L., JR. and MCGEE J. J. (1979) Thermal and mechanical history of granulated norite and pyroxene anorthosite clasts in breccia 73255. *Proc. Lunar Planet. Sci. Conf. 10th* **1,** 817–832.

OSTERTAG R. (1981) Annealing experiments on experimentally shocked feldspar single crystals. *Meteoritics* **16,** 373.

PRICE G. D., PUTNIS A. and AGRELL S. O. (1979) Electron petrography of shock-produced veins in the Tenham chondrite. *Contrib. Mineral. Petrol.* **71,** 211–218.

RALEIGH C. B., KIRBY S. H., CARTER N. L. and AVE LALLEMANT H. G. (1971) Slip and the clinoenstatite transformation as competing rate processes in enstatite. *J. Geophys. Res.* **76,** 4011–4022.

RAMDOHR P. (1973) *The Opaque Minerals in Stony Meteorites.* Amsterdam: Elsevier.

REID A. M. and COHEN A. J. (1967) Some characteristics of enstatite from enstatite chondrites. *Geochim. Cosmochim. Acta* **31,** 661–672.

REIMOLD W. U. and STOFFLER D. (1978) Experimental shock metamorphosis of dunite. *Proc. Lunar Planet. Sci. Conf. 9th* **2,** 2805–2824.

ROSS J. V. and NIELSEN K. C. (1978) High-temperature flow of wet polycrystalline enstatite. *Tectonophysics* **44,** 233–261.

SCHAAL R. B., HORZ F., THOMPSON T. D. and BAUER J. F. (1979) Shock metamorphism of granulated lunar basalt. *Proc. Lunar Planet Sci. Conf. 10th* **3,** 2547–2571.

SCHNEIDER H. (1977) Mechanical deformation and structural state of experimentally shock-loaded oligoclases. *Neues Jahrb. Miner. Mh.* **1977,** 255–269.

SEARS D. W. (1980) Thermoluminescence of meteorites: Relationships with their K-Ar age and their shock and reheating history. *Icarus* **44,** 190–206.

SEARS D. W. and MARSHALL C. (1980) Some studies on magnetic extracts from unequilibrated ordinary chondrites. *Meteoritics* **15,** 364–365.

SEARS D. W., GROSSMAN J. N., MELCHER C. L., ROSS L. M. and MILLS A. A. (1980) Measuring the metamorphic history of unequilibrated ordinary chondrites. *Nature* **287,** 791–795.

SMITH B. A. and GOLDSTEIN J. I. (1977) The metallic microstructures and thermal histories of severely reheated chondrites. *Geochim. Cosmochim. Acta* **41,** 1061–1072.

STOFFLER D. (1974) Deformation and transformation of rock-forming minerals by natural and experimental shock processes. II. Physical properties of shocked minerals. *Fortschr. Miner.* **51,** 256–289.

STOFFLER D. and HURNEMANN U. (1972) Quartz and feldspar glasses produced by natural and experimental shock. *Meteoritics* **7,** 371–394.

TAYLOR G. J. and HEYMANN D. (1969) Shock, reheating and the gas retention age of chondrites. *Earth Planet. Sci. Lett.* **7,** 151–161.

TAYLOR G. J. and HEYMANN D. (1970) Electron microprobe study of metal particles in the Kingfisher meteorite. *Geochim. Cosmochim. Acta* **34,** 677–687.

TAYLOR G. J. and HEYMANN D. (1971) Post-shock thermal histories of reheated chondrites. *J. Geophys. Res.* **76,** 1879–1893.

TURNER G., ENRIGHT M. C. and CADOGAN P. H. (1978) The early history of chondrite parent bodies inferred from ^{40}Ar-^{39}Ar ages. *Proc. Lunar Sci. Conf. 9th,* 989–1025.

WEGNER M. W. and CHRISTIE J. M. (1974) Preferential chemical etching of terrestrial and lunar olivines. *Contrib. Mineral. Petrol.* **43,** 195–212.

WOOD J. A. (1967) Chondrites: Their metallic minerals, thermal histories, and parent planets. *Icarus* **6,** 1–49.

ZUKAS E. G. (1969) Metallurgical results from shock-loaded iron alloys applied to a meteorite. *J. Geophys. Res.* **74,** 1993–2001.